

## Rapid thermal oxidation of nano silver film for solar cell fabrication

M. A. Fakhri<sup>a,b,\*</sup>, R. A. Basheer<sup>c</sup>, A. M. Banoosh<sup>c</sup>, H. N. Azeez<sup>c</sup>

<sup>a</sup>Laser and Optoelectronic Engineering Department, University of Technology-Iraq, Baghdad, Iraq

<sup>b</sup>Institute of Nano Electronic Engineering, University Malaysia Perlis, 01000 Kangar, Perlis, Malaysia

<sup>c</sup> Department of Physics, College of Education, University of Al-Hamdaniya, Nineveh, Iraq

In this paper, the nano Silver dioxides films have been deposited using the reactive pulsed laser deposition method (RPLD) using the tattoo removal Q-switching Nd-Yag laser, at the value of the wavelength of 1064nm, pulseduration of 6 sec, and 800 mJ energy of laser have been applied for ablated an extra purity of the Silver target then deposited the nano silver oxide particles on the silicon substrates, synthesize and studying of the rapid thermal annealing (RTA) effects on the structural properties, the morphological properties, the Optical properties, the electrical properties and finally the solar cell properties for the prepared samples. Both X-ray diffraction and electron microscopy studies show that the structure of the film depends on the annealing temperatures effects of the deposited film. The nano silver oxide is present in different crystalline stages, where the particle sizes have been increases with increasing heat treatment from 45nm to 75 nm. The analyzed Results of the optical approve the improvements of the absorption lead to decreasing the reflection values compared with the surface of the silicon (crystalline Si), where the transparency for the range of larger than 300 nm and the values of the optical band gap of 2.12 eV. The synthesized results for the solar cell fabrications present a clear improvement in the solar cell quantum efficiency values in the case of silver nano oxide deposition and annealed with the high degree, where the value of the efficiency about of 4.22.

(Received December 17, 2020; Accepted April 2, 2021)

**Keywords:** RPLD, Ag<sub>2</sub>O, Surface morphology, Solar cell properties, Optical properties, Nano silver

### 1. Introduction

Silver oxygen is the chemical substance (Ag-O) and it is a black or dark brown fine powder used in preparing other silver compounds [1-4]. Silver nanooxides are p-type semiconductor materials with energy band gaps ranging from 1.2 eV to 3.4 eV [5-9]. These nanoparticles are known in several forms: Ag<sub>2</sub>O, AgO, Ag<sub>3</sub>O<sub>4</sub>, Ag<sub>4</sub>O<sub>3</sub>, Ag<sub>2</sub>O<sub>3</sub> and Ag<sub>4</sub>O<sub>4</sub>, and this oxide are used in silver-oxide batteries [10-13]. Where laboratory and practically the two compounds Ag<sub>2</sub>O and AgO silver oxides are the most stable of the previously mentioned group of oxides [14-18].

The stability, structure, size, morphology, and properties of nanostructures depend on the various compositional methods and criteria used [19-22]. The nano silver oxide films in organic chemistry are used as an agent oxidizing light. i.e, that is, it works by oxidizing aldehydes to carboxylic acids [23-25]. These reactions are used effectively when preparing silver oxides in situ and in laboratories from mixing alkali hydroxides and silver nitrate. A conventional solar cell, a portion of the solar energy that falls on photovoltaics is wasted in the form of untapped thermal energy discovered and used by humans. For this reason, nanotechnology that uses thin films is used [26-28].

---

\* Corresponding authors: makram.a.fakhri@uotechnology.edu.iq.

Nanotechnology has contributed to creating a number of unique and technological solutions, especially in the field of solar cells production, as it works to raise energy efficiency and reduce the cost of its production and operation to suit all applications to suit all life and industrial applications. Several methods have been adopted for preparing and depositing these nanoparticles [29-31]. These include: the reduction of the chemical by using the organic varieties and the factors reducing non-organic [32, 33], methods of the electrochemical [34, 35], and Physical chemical reduction [36, 37]. Many modern and varied techniques have been used to prepare silver oxide nanofilms. These techniques such as the Evaporation of the RF[38], the Evaporation of the electron beam [39], the chemical bath deposition [40], the pulsed laser deposition [41], and the pulsed laser ablation in liqueds [42] etc.

Silver Oxides nanoparticles are used in inorganic chemistry as a light oxidizing agent. For example, it oxidizes aldehydes into carboxylic acids. Often these reactions work best when silver nanoxides are prepared in situ and in laboratories with silver nitrate and also with alkali hydroxide as cofactors [43-45].

In this presented paper, rapid thermal annealing has been achieved and its effects on the physical properties for the deposited Nano silver oxides for fabricated the solar cells. The quantitative efficiency, the filling factor, and other variables were tested and discussed the presented results.

## 2. Experimental

In this paper, the effects of rapid thermal annealing on the structural, morphological, optical, electrical, and solar cell properties for the deposited nanosilver oxides film have been studied in this manuscript. Where it is possible to control the transparency and conductivity of the deposited films by fixing and changing the conditions of sedimentation to enable us to use these nanofilms in photonics and optical-electronic applications.

A system of the laser Q-switching Tattoo removal Nd-YAG has been used for ablated the extra purity of Silver metal target on the substrates of Si at 350 °C, a photograph shows the PLD system parts are presents in figure (1) [46, 47].



*Fig. 1 the system of the pulse laser deposition (pld)*

An extra purity (99.999%) Silver metals powders have been supplied from the Fluka company was used to production the Ag target at disk diameter = 20 mm and the thickness of 5 mm under the pressing force of 10 ton. The substrates samples (samples of silicon) are formed (Been sliced) up square-shaped of 1.5x1.5 cm by using a wire-cut machine. The film was performed deposition usually in the background ambient oxygen gas (O<sub>2</sub>) pressure of up to 350000 mTor. It was allowed to enter this background gas to the discharge chamber through the needle valve.

The nano thin layer was immediately achieved upon the beam of the pulsed laser hitting the target resulting in the ablation of the target material, which is based on the rotating motor with the angle of 45 ° from the substrate to ensure that the plasma column falls and precipitates directly

onto the substrate. As the process of using target rotation to ensure that ablation does not occur in the same place on the target being used, the distance between the substrate and the target is approximately 30 mm.

Keithley devices have been used to test the flowing current in the fabricated structure of the solar cell produced in the state of dark and the formed voltage from the power source ranges (500-3000) mV in forward bias, and (500-5000) mV in the biasing of reverse. A fairly thick layer of high-purity aluminum was deposited at the top and back of the fabricated device as an ohmic contact.

The C-V measurements have been tested using the programmable LRC meter model of PM6306 scale programmable and supplied by Fluke, at the reverse voltage bias at the range of (500-5000) mV. The value of the point cross ( $1/C^2=0$ ) from the curve ( $1/C^2-V$ ) represents the built-in potential of the nano heterostructure [48-50].

The values of the responsivity and the spectral response results have been tested using a double-beam spectrometer at the range of work about wavelengths of (150-1100) nanometers, and the measurements of the voltage-current have been tested by a digital multimeter from Fluke. The responsivity and the spectral response have been analyzed using the following formula [51-53]:

$$R_{\lambda} = \frac{I_{ph}}{P_i} \quad \text{A/W} \quad (1)$$

where  $I_{ph}$  refers to the values of the measured photoelectric current and  $P_i$  is the value of the incident optical power.

The quantitative efficiency value was also calculated based on the formula [54, 55]:

$$\eta = 1.24 \frac{R_{\lambda}}{\lambda} \quad (2)$$

The values of the efficiency and the factor of the filling for the fabricated solar cell have been tested by placing it under the 100 mW/cm<sup>2</sup> tungsten lamp illumination and it 120 mm away placed.

The factor of the fill (FF) have been tested for the quality junction and the resistance series for the cell, and it's defined as: [56-58]

$$FF = \frac{V_{mp} I_{mp}}{V_{oc} I_{sc}} \quad (3)$$

The values of the quantum efficiency for the fabricated solar cell was tested as the fraction of power incident (light) that are converted to electricity and its formula are:

$$\eta = \frac{P_{max}}{P_{inc}} \quad (4)$$

where  $P_{max} = V_{oc} I_{sc} FF$

where  $V_{oc}$  is the voltage at the open-circuit; and the  $I_{sc}$  its the current in the short-circuit [22].

The setup of the experimental is schematically illustrated in the presented figure (2).

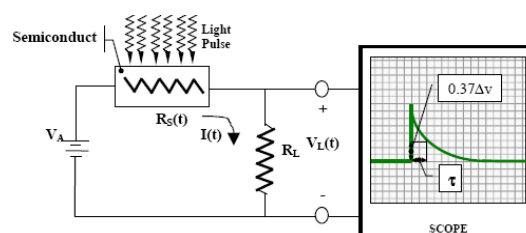


Fig. 2. The setup of the Experimental for the measurement of the carrier life time.

### 3. Result and discussion

#### 3.1. Structural properties

Figure 3 presents the diffractions of the X-ray profiles for the nanosilver oxide structures treated at 400 and 500 °C annealing temperatures and 120 sec time of oxidation. The nano-thin films deposited and treated show three different peaks presented at the  $2\theta$  = 33.18°, 38.75°, and 67.17° that are related to the diffraction planes of (111), (200), and (103) respectively, all these peaks appear in the both of the annealing treated and also all are represent to the nanosilver oxides. The plane (111) is representing the strong reflection peak along comparing with the other reflections of (200) and (103), this corresponds to the single-phase  $\text{Ag}_2\text{O}$  growth with shape structure of cubic. It is clearly that, the peak intensity for the deposited and treated structures at 500 °C are higher than that deposited and treated structures at 400 °C, This apparent difference is the result of a better crystallization at a temperature of 500 °C, as well as a clear improvement in the crystal structure of the silver oxide nanostructures, and an indication of complete oxidation of the stripped silver crystals from the original target used, This interpretation matches previous publications [48]

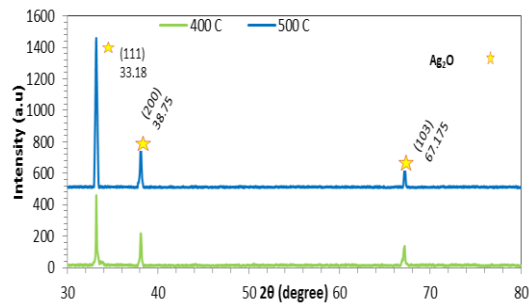


Fig. 3. XRD pattern of nanosilver oxides treated at different temperatures.

#### 3.2. Optical properties

Figure 4 presents the optical spectra transmission for the nanosilver oxides films deposited and treated at different heat treatments. It is clear that the nano deposited and treated films gives high and good transparency values at the range of the spectral about the 0.4-0.8 micrometer, Where the transmission values range are reduction from (90% to 77%) with the increasing the heat treated from 400 to 500 °C respectively. The lower permeability value within the UV region is related to the value of the optical energy gap of the precipitated nanomaterial that is present within this region as part of the physical properties of this nanomaterial. Within the visible range of wavelengths, higher optical transmittance values indicate low surface roughness and good homogeneity of the deposited nanofilm [42].

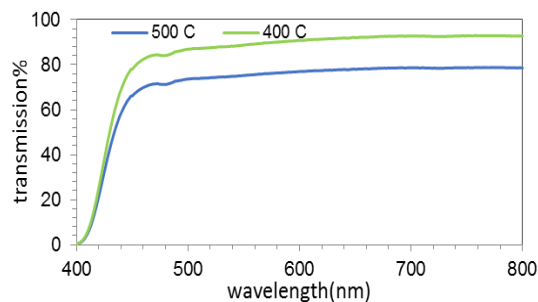


Fig 4. Spectra of the optical transitions for nano silver oxides films treated at different temperatures.

The values of the optical band gap ( $E_g$ ) for the nano deposited and treated films were predestined computed from plots of the photon energy ( $h\nu$ ) versus the  $(\alpha h\nu)^2$  by using the relation of extrapolation for the linear portion of the  $(\alpha h\nu)^2$  versus photon energy curve to the  $\alpha = 0$  resulting the optical energy band gap values of the deposited and treated nano silver oxides films as presented in fig. 5. The values of the optical energy band gap for the deposited and treated nano silver oxides films have been increased from 2.095 to 2.122 eV with increase of the heat treated, and this increase as a result of increasing of the sizes of grains for the deposited and treated nano silver oxides films with increase of the heat treated, and this lead to a redshift. The optical energy band gap values reported for the silver oxide nanofilms varied depending on the different deposition methods used and the parameters of the different deposition processes that are changed to ensure the growth of the nanofilm.

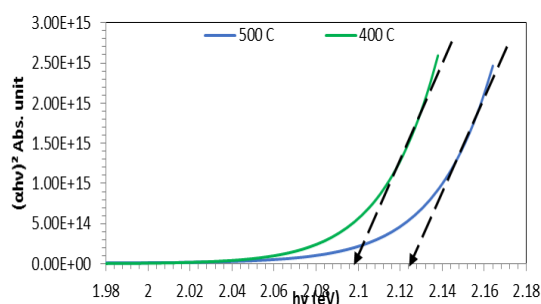


Fig. 5. Optical band gap for nano silver oxides films treated at different temperatures.

### 3.3. Morphological properties

Figure 6 displays the results of the morphological nanostructure of the precipitated and heat treated silver oxides. The uniform distribution of the nanoparticles is quite clear in the images shown in the figure, and the difference in the particle sizes can be observed according to the heat treatment. As for the silver oxidation nanoparticles deposited and heat treated at 400 ° C, it appears clearly that the number of nanoparticles with spherical shape and uniform distribution, and the average sizes of these nanoparticles were about 45 nm. The concentration of nanofilms of silver oxides increases with increasing heat treatment to 400 ° C, in addition to increasing the size of nanoparticles to about 75 nm. The SEM images confirm that the increase in the number and sizes of the nanoparticles at the higher thermal treatment of 500 ° C is the reason for the further reduction of the energy of the incident optical beam, which leads to an increase in the particle size.

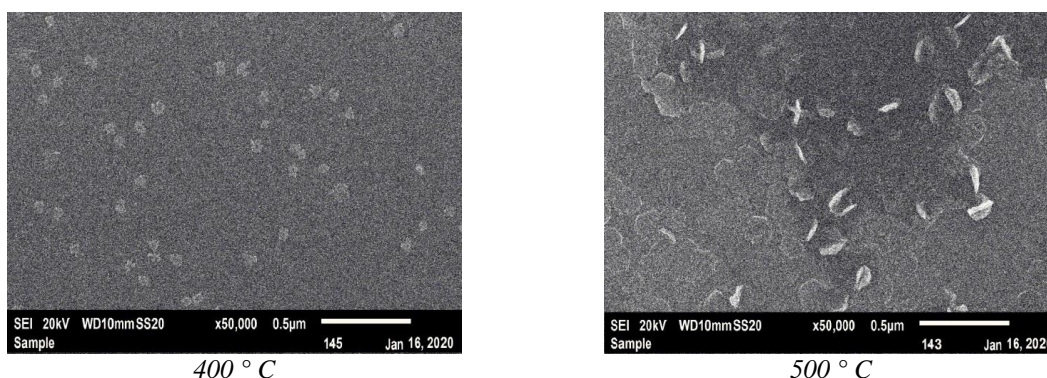


Fig. 6. FESEM image for nano silver oxides films treated at different temperatures.

This examination is considered one of the most important tests for the deposited nanofilms for the purpose of using it in the synthesis of optical and electro-optical devices as it works to determine various key parameters such as potential capacity of the device and the type of device,

as Figure (7) presents the CV measurements of the silver oxidation nanofilms that have been deposited and treated thermally. The results showed in the figure below that the capacitance value of the device is inversely proportional to the bias voltage value for both prepared samples. The value of the decrease in the capacitance value of the prepared devices with increasing the bias voltage is caused by the expansion in the depletion region with the value of the barrier potential. The value of the depletion area amplitude indicates an increase in the values of the charge per unit area and a gradual change in the applied voltage. As this characteristic gives a clear indication of the behavior of the transport and movement of shipments from the donor area to the receiving party, as it was found to be of the "sudden" type and confirms this behavior when the relationship is linear and straight between  $1 / C^2$  and reverse bias.

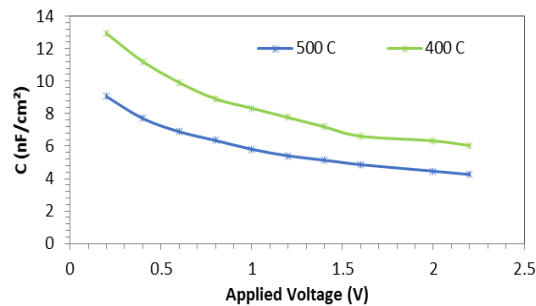


Fig. 7.  $c$ - $v$  characteristics for nano silver oxides films treated at different temperatures.

Figure 7 shows the relationship between the square capacitance versus the reverse bias voltage diagram mathematically computed from the C-V properties as shown in the previous result above. The linear relationship of the  $1 / C^2$  - $V$  curve indicates that the prepared and thermally treated silver oxides of silver are of the abrupt type, and that the intercept value of  $1 / C^2$  with the applied voltage is the diffusion potential. It clearly shows that the higher thermal treatment of 500 degrees Celsius works better and gives higher and better results because its structural, topographical, optical and physical properties, according to what was previously presented, are better than samples that have been thermally treated with a value of less than 400 degrees Celsius, and this has the effect of utilizing the largest energy to convert Light into electricity according to the photoelectric phenomenon, due to the higher crystallization.

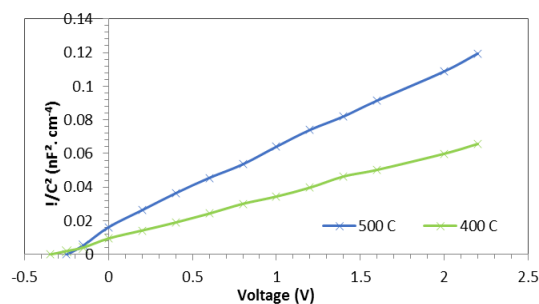


Fig. 8.  $1/c^2$  - $v$  characteristics for nano silver oxides films treated at different temperatures.

Fig. 9 shows the relationship between  $V_{oc}$  and  $I_{sc}$  as a function of the load variable resistance. The efficiency of the blocking and deposited device in both cases was calculated at the heat treatment values of 400 and 500 ° C for comparison. Where the quantitative efficiency values were (2.86 and 4.22) respectively, that is, there is a marked improvement in the quantitative efficiency values of devices prepared from the precipitation of nanostructured silver oxides and heat treated at a higher temperature, where the reason is due to the absorption values.

At the surface of the nanoparticles and at the separating region (the first junction formed between the silver oxide nanolayer and the surface of the silicon base).

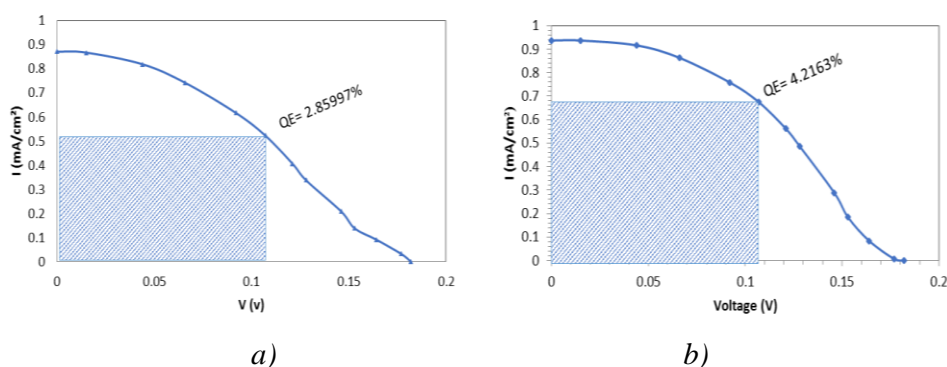


Fig. 9. Quantum efficiency for Ag<sub>2</sub>O/Si solar cell at two different laser wavelengths. a) 400 °C , b) 500 °C

#### 4. Conclusion

Silver oxide Nano structure film have been deposited successfully by using the (RPLD) reactive pulsed laser deposition technique on the substrates of silicon and it have been treated heatly at two differente heat treatments ( 400 and 500 ° C ). The structural reslts present a three different peaks at the 2 thetas = 33.18°, 38.75°, and 67.17° that are related to the diffraction planes of (111), (200), and (103) respectively, for both of the heat treated and the plane (111) is representing the strong reflection peak and also it is clearly that, the peak intensity for the deposited and treated structures at 500 °C are higher than that deposited and treated structures at 400 °C. The Optical results presents a good value of the transparency for the range of larger than 300 nm and the values of the optical band gap of 2.12 eV. The value of the efficiency for the deposited and treated hetely device present a difference in both cases of (4.22, 2.86) respectively.

#### References

- [1] A. H. Hammad, M. S. Abdel-Wahab, A. Alshahrie, Digest Journal of Nanomaterials and Biostructures **11**(4), 1245 (2016).
- [2] H. M. Ahmed, M. J Abdul Razzaq, A. K Abass, Int. J. Nanoelectron. Mater **11**, 473 (2018).
- [3] M. A. M. Hassan, M. F. H. Al-Kadhemy, E. T. Salem, International Journal of Nanoelectronics and Materials **8**(2), 69 (2014).
- [4] W. Wu, C. C. Tseng, C. Li, C. K. Chang, J. H. Hsieh, Vacuum **118**, 147 (2015).
- [5] M. J. AbdulRazzaq, A. Z Mohammed, A. K Abass, K. S Shibib, Optical and Quantum Electronics **51**(9), 294 (2019).
- [6] M. T. Awayiz, E. T Salim, AIP Conference Proceedings **2213**(1), 020247 (2020).
- [7] M. Y. Ghadban, K. S Shibib, M. J. Abdulrazzaq, AIP Conference Proceedings **2213**(1), 020179 (2020).
- [8] L. A. A. Pettersson, P.G. Snyder, Thin Solid Films **270**, 69 (1995).
- [9] M. A Dawood, M. A Fakhri, F. G Khalid, O. S Hassan, M. S Abdulla, A. A. Ahmed, S. A. Abduljabar, IOP Conference Series: Materials Science and Engineering **454**(1), 012161 (2018).
- [10] T. C. Kaspar, T. C. Droubay, S. A. Chambers, Thin Solid Films **519**, 635 (2010).
- [11] C. C. Tseng, J. H. Hsieh, W. Wu, Thin Solid Films **519**, 5169 (2011).
- [12] A. Kadhim, E. T. Salim, S. M. Fayadh, A. A. Al-Amiery, A. H. Kadhum, A. B. Mohamad, The Scientific World Journal, 2014 (2014) Article ID 490951, 6 pages.
- [13] E. Lund, A. Galeckas, A. Azarov, E. V. Monakhov, Thin Solid Films **536**, 156 (2013).

- [14] Y. You, L. Wan, S. Zhang, D. Xu, *Materials Research Bulletin* **45**, 1850 (2010).
- [15] Z. T. Salim, U. Hashim, M. K. Md. Arshad, Makram A. Fakhri, Evan T. Salim, *Materials Research Bulletin* **86**, 215 (2017).
- [16] K. Lalitha, J. K. Reddy, M. V. P. Sharma, V. D. Kumari, M. Subrahmanyam, *International Journal of hydrogen energy* **35**, 3991 (2010).
- [17] Jonathan Derouin, Rachael G. Farber, Stacy L. Heslop, Daniel R. Killelea, *Surface Science* **641**, L1 (2015).
- [18] M. A. Fakhri, N. H. Numan, Q. Q. Mohammed, M. S. Abdulla, O. S. Hassan, S. A. Abduljabar, A. A. Ahmed, *International Journal of Nanoelectronics and Materials* **11** (Special Issue BOND21), 109 (2018).
- [19] X. Gao, S. Wang, J. Li, Y. Zheng, R. Zhang, P. Zhou, Y. Yang, L. Chen, *Thin Solid Films* **455-456**, 438 (2004).
- [20] F. X. Bocka, T. M. Christensen, S. B. Rivers, L. D. Doucette, R. J. Lada, *Thin Solid Films* **468**, 57 (2004).
- [21] E. T. Salim, M. T. Awayiz, R. O. Mahdi, *Digest Journal of Nanomaterials and Biostructures* **14**(4), 1151 (2019).
- [22] S. B. Rivers, G. Bernhardt, M. W. Wright, D. J. Frankel, M. M. Steeves, R. J. Lad, *Thin Solid Films* **515**, 8684 (2007).
- [23] G. Xiaoyong, Z. Mengke, Z. Zengyuan, C. Chao, M. Jiaomin, L. Jingxiao, *Thin Solid Films* **519**, 6620 (2011).
- [24] M. K. Abood, M. Halim, A. Wahid, E. T. Salim, J. Admon, *The European Physical Journal Conferences* **162**(12), 01058 (2017).
- [25] Z. Meng-Ke, L. Yan, G. Xiao-Yong, C. Chao, C. Xian-Mei, Z. Xian-Wei, *Chin. Phys. B* **21**(6), 066101 (2012).
- [26] B. Chiyah, Kamal Kayed, *International Journal of Nanoelectronics and Materials* **11**(3), 305 (2018).
- [27] M. A. Fakhri, A. W. Abdulwahhab, M. A. Dawood, A. I. Sabah, *AIP Conference Proceedings* **2213**(1), 020226 (2020).
- [28] J. Tominaga, *Journal of Physics Condensed Matter* **15**(25), R1101 (2003).
- [29] G. Benetti, Emanuele Cavaliere, Francesco Banfi, Luca Gavioli, *Materials* **13**, 784 (2020).
- [30] M. Talib Awayiz, E. T. Salim, *Materials Science Forum* **1002**, 200 (2020).
- [31] I. A. Hamad, R. I. Khaleel, A. M. Raoof, *Baghdad Science Journal* **16**(4), 1036 (2019).
- [32] C. Persson, S. Mirbt, *Braz. J. Phys.* **36**(2A), 286 (2006).
- [33] H. Asady, E. T. Salim, R. A. Ismail, *AIP Conference Proceedings* **2213**(1), 020183 (2020).
- [34] F. A. Kiani, U. Shamraiz, Amin Badshah, *Mater. Res. Express* **7**, 015035 (2020).
- [35] A. C. Nwanya, P. E. Ugwuoke, B. A. Ezekoye, R. U. Osuji, F. I. Ezema, *Advances in Materials Science and Engineering*. **2013**, 450820 (2013).
- [36] F. A. Hattab, M. A. Fakhri, F. G. Khalid, L. F. Awni, S. A. Ali, G. Q. Ramzi, A. I. Hussien, *AIP Conference Proceedings* **2213**(1), 020243 (2020).
- [37] M. A. Fakhri, M. Halim A. Wahid, B. A. Badr, E. T. Salim, U. Hashim, Z. T. Salim, *The European Physical Journal Conferences* **162**(7), 01004 (2017).
- [38] H. H. Hassen, E. T. Salim, J. M. Taha, R. O. Mahdi, N. H. Numan, F. G. Khalid, M. A. Fakhri, *International Journal of Nanoelectronics and Materials* **11**(Special Issue BOND21), 65 (2018).
- [39] E. T. Salim, A. I. Hassan, S. A. Naaes, *Materials Research Express* **6**(8), 086416 (2019).
- [40] A. D. Faisal, R. A. Ismail, W. K. Khalef, E. T. Salim, *Optical and Quantum Electronics* **52**, 1 (2020).
- [41] M. Abood, E. T. Salim, J. A. Saimon, *Journal of Ovonic Research* **15**(2), 109 (2019).
- [42] E. T. Salim, R. A. Ismail, M. A. Fakhri, B. G. Rasheed, Z. T. Salim, *Iranian Journal of Science and Technology, Transactions A: Science* **43**(3), 1337 (2019).
- [43] M. Abdul Muhsien, E. T. Salim, Y. Al-Douri, A. F. Sale, I. R. Agool, *Applied Physics A: Materials Science and Processing* **120**(2), 725 (2015).
- [44] E. T. Salim, Y. Al-Douri, M. S. Al Wazny, M. A. Fakhri, *Solar Energy* **107**, 523 (2014).
- [45] E. T. Salim, *Surface Review and Letters* **20**(05), 1350046 (2013).
- [46] M. A. Fakhri, M. Halim A. Wahid, S. M. Kadhim, B. A. Badr, E. T. Salim,

- U. Hashim, Z. T. Salim, The European Physical Journal Conferences **162**, 01005 (2017).
- [47] S. A. Naayi, A. I. Hassan, E. T. Salim, International Journal of Nanoelectronics and Materials **11**(Special Issue BOND21), 1 (2018).
- [48] M. A. Fakhri, E. T. Salim, U. Hashim, A. W. Abdulwahhab, Z. T. Salim, Journal of Materials Science: Materials in Electronics **28**(22), 16728 (2017).
- [49] E. T. Salim, M. A. Fakhri, H. Hassen, International Journal of Nanoelectronics and Materials **6**(2), 121 (2013).
- [50] M. A. Fakhri, M. M. Hassan, AIP Conference Proceedings **2213**(1), 020244 (2020).
- [51] M. A. Fakhri, U. Hashim, E. T. Salim, Z. T. Salim, Journal of Materials Science: Materials in Electronics **27**(12), 13105 (2016).
- [52] S. Sagadevan, Int. J. Nanoelectronics and Materials **9**, 37 (2016).
- [53] E. T. Salim, M. S. Al-Wazny, M. A. Fakhri, Modern Physics Letters B **27**(16), 1350122 (2013).
- [54] E. T. Salim, H. T Halboos, Materials Research Express **6**(6), (0664012019).
- [55] M. A. Fakhri, E. T. Salim, M. H. A. Wahid, U. Hashim, Zaid T. Salim, Journal of Materials Science: Materials in Electronics **29**(11), 9200 (2018).
- [56] M. A Fakhri, M. J. AbdulRazzaq, A. A. Alwahib, W. H Muttalak, Optical Materials **109**, 110363 (2020).
- [57] E. T. Salim, International Journal of Nanoelectronics and Materials **5**(2), 95 (2012).
- [58] F. G. Khalid, A. S. Ibraheam, M. A. Fakhri, N. H. Numan, AIP Conference Proceedings **2213**(1), 020204 (2020) .